

# A time splitting method for the three-dimensional linear Pauli equation

Timon S. Gutleb<sup>a,b,\*</sup>, Norbert J. Mauser<sup>a</sup>, Michele Ruggeri<sup>c</sup>, Hans-Peter Stimming<sup>a</sup>

<sup>a</sup>WPI c/o Fak. Mathematik, Universität Wien, A1090 Vienna

<sup>b</sup>Dept. of Mathematics, Imperial College London, SW7 2AZ, UK

<sup>c</sup>Inst. for Analysis and Scientific Computing, TU Wien, A1040 Vienna

---

## Abstract

We present and analyze a numerical method to solve the time-dependent linear Pauli equation in three space-dimensions. The Pauli equation is a "semi-relativistic" generalization of the Schrödinger equation for 2-spinors which accounts both for magnetic fields and for spin, the latter missing in preceeding work on the linear magnetic Schrödinger equation. We use a four operator splitting in time, prove stability and convergence of the method and derive error estimates as well as meshing strategies for the case of given time-independent electromagnetic potentials (= "linear" case), thus providing a generalization of previous results for the magnetic Schrödinger equation. Some proof of concept examples of numerical simulations are presented.

*Keywords:* Pauli equation, operator splitting, time splitting, magnetic Schrödinger equation,

semi-relativistic quantum mechanics

*2010 MSC:* 35Q40, 35Q41, 65M12, 65M15

---

## 1. Introduction

Relativistic quantum mechanics is appropriate for the dynamics of "fast" charged particles (e.g. electrons moving close to speed of light  $c$ ). In the *fully relativistic regime* the Dirac equation with electromagnetic potentials is the appropriate model, where the unknown is a 4-spinor including both spin and antimatter in a quantum field theory approach [1, 2].

In the *fully non-relativistic* ("Newtonian")  $c \rightarrow \infty$  regime one uses the standard Schrödinger equation with electric potential for the scalar wave function.

In the intermediate *semi-relativistic* ("Post-Newtonian") regime of a first order theory, i.e. keeping the corrections at  $O(\frac{1}{c})$ , the appropriate model is the Pauli equation for the 2-spinor. It is the simplest available theory that retains relativistic effects of both electromagnetism *and* spin, in contrast to the scalar magnetic Schrödinger equation where spin is completely absent in the model.

---

\*Corresponding author

Email addresses: [t.gutleb18@imperial.ac.uk](mailto:t.gutleb18@imperial.ac.uk) (Timon S. Gutleb), [norbert.mauser@univie.ac.at](mailto:norbert.mauser@univie.ac.at) (Norbert J. Mauser), [michele.ruggeri@asc.tuwien.ac.at](mailto:michele.ruggeri@asc.tuwien.ac.at) (Michele Ruggeri), [hans.peter.stimming@univie.ac.at](mailto:hans.peter.stimming@univie.ac.at) (Hans-Peter Stimming)

This hierarchy of approximations of the Dirac equation is laid out, e.g. in [2, 3, 4] and in [3, 4] specifically also for the self-consistent case of coupling to the Maxwell equations.

The Pauli equation contains a magnetic Schrödinger operator and a so-called Stern-Gerlach term that couples the magnetic field to the spin operators; the time dependent version reads:

$$i\hbar\partial_t u = \left[ \frac{1}{2m} \left( -i\hbar\nabla - \frac{q}{c}\mathbf{A} \right)^2 + q\phi - \frac{\hbar q}{2mc} \boldsymbol{\sigma} \cdot \mathbf{B} \right] u. \quad (1)$$

Here,  $u \in \mathbb{C}^2$  is a 2-spinor  $(u_1, u_2)^T$  representing quantum mechanical spin up and spin down states,  $\mathbf{A} \in \mathbb{R}^3$  and  $\phi \in \mathbb{R}$  denote the magnetic vector potential and the electric scalar potential, respectively, which are related to the electromagnetic fields by

$$\mathbf{E} = -\nabla\phi - \partial_t \mathbf{A} \quad \text{and} \quad \mathbf{B} = \nabla \times \mathbf{A}.$$

Moreover,  $i \in \mathbb{C}$  denotes the imaginary unit, i.e.,  $i^2 = -1$ ,  $\boldsymbol{\sigma} = (\sigma_1, \sigma_2, \sigma_3)$  is a vector collecting the 3 Pauli matrices

$$\sigma_1 = \begin{pmatrix} 0 & 1 \\ 1 & 0 \end{pmatrix}, \quad \sigma_2 = \begin{pmatrix} 0 & -i \\ i & 0 \end{pmatrix}, \quad \text{and} \quad \sigma_3 = \begin{pmatrix} 1 & 0 \\ 0 & -1 \end{pmatrix},$$

and the product  $\boldsymbol{\sigma} \cdot \mathbf{B}$  is a shorthand notation for the matrix

$$\boldsymbol{\sigma} \cdot \mathbf{B} = \sum_{j=1}^3 B_j \sigma_j = \begin{pmatrix} B_3 & B_1 - iB_2 \\ B_1 + iB_2 & -B_3 \end{pmatrix} \in \mathbb{C}^{2 \times 2}.$$

Finally,  $m$  and  $q$  are the associated mass and charge, while the positive constants  $\hbar$  and  $c$  are the scaled Planck constant and the speed of light respectively. The above rendition of the Pauli equation retains all of the gauge freedom of electrodynamics and is semi-relativistic in the sense that it is suitable for medium high velocities relative to the speed of light, cf. [3, 4].

From the complex valued 2-spinor solution  $u$  of (1) the physical quantities of interest are computed as "quadratic quantities", e.g. the position density  $n = |u|^2 = u \cdot \bar{u}$  and the current density<sup>1</sup> which contains (divergence free) extra terms to the standard definition for the Schrödinger equations (cf. [5]),

$$\mathbf{J} = -\frac{i\hbar}{2m}(\bar{u} \cdot \nabla u - u \cdot \nabla \bar{u}) - \frac{q}{mc}|u|^2 \mathbf{A} - \frac{|q|\hbar}{2m} \nabla \times (\bar{u} \boldsymbol{\sigma} u). \quad (2)$$

The continuity equation connects  $n$  and  $\mathbf{J}$  as

$$\partial_t n + \nabla \cdot \mathbf{J} = 0,$$

also conservation of total mass holds

$$m_{\text{tot}} = m \int_{\mathbb{R}^3} n \, d\mathbf{x} = m \int_{\mathbb{R}^3} |u|^2 \, d\mathbf{x},$$

---

<sup>1</sup>In (2),  $\bar{u} \cdot \nabla u = \bar{u}_1 \nabla u_1 + \bar{u}_2 \nabla u_2 \in \mathbb{R}^3$  and  $u \nabla \bar{u} = u_1 \nabla \bar{u}_1 + u_2 \nabla \bar{u}_2 \in \mathbb{R}^3$ , while  $\bar{u} \boldsymbol{\sigma} u \in \mathbb{R}^3$  denotes the vector with components  $(\bar{u} \boldsymbol{\sigma} u)_j = \bar{u} \sigma_j u$  for all  $j = 1, 2, 3$ .

and conservation of the total energy of both components of the 2-spinor:

$$\mathcal{E} = \frac{1}{2m} \int_{\mathbb{R}^3} |(-i\hbar\nabla - (q/c)\mathbf{A})u|^2 dx + q \int_{\mathbb{R}^3} \phi|u|^2 dx - \frac{\hbar q}{2mc} \int_{\mathbb{R}^3} (\boldsymbol{\sigma} \cdot \mathbf{B})u \cdot \bar{u} dx.$$

In this paper, we propose and analyze an exponential splitting method [6] for the Pauli equation (1). The scheme is an extension of analogous approaches developed for the scalar magnetic Schrödinger equation [7, 8, 9]. Our method consists of a four-term operator splitting, where the three operator contributions appearing in the magnetic Schrödinger equation (kinetic, potential, advective) are supplemented with a fourth term accounting for spin. The presence of this additional contribution determines also a bidirectional coupling of the two equations for the two components of  $u$ .

The remainder of this paper is organized as follows: The proposed method is described in Section 2; The applicability of the scheme is demonstrated in Section 3, where we show proof of concept numerical experiments; In Section 4 we study stability (Theorem 4.5) and convergence (Theorem 4.6) of the method; Finally, in Section 5, we summarize the results and provide a short outlook on possible further generalizations of the present work.

## 2. A four-term exponential splitting scheme

We first "rescale" the Pauli equation (1) into a non-dimensionalized form which is more suitable for the presentation of the splitting method and its analysis, and discuss some properties of the equation. We chose the non-dimensionalization such that the Pauli equation takes "semi-classical" form<sup>2</sup>

$$i\varepsilon \partial_t u = \left[ \frac{1}{2}(-i\varepsilon \nabla - \mathbf{A})^2 - \frac{\varepsilon}{2} \boldsymbol{\sigma} \cdot \mathbf{B} + \phi \right] u, \quad (3)$$

where the one dimensionless parameter  $\varepsilon$  is proportional to  $\frac{\hbar}{c}$ , so it is related both to the semi-classical and the non-relativistic scale. The rescaled magnetic field and potentials (not relabeled) are also dimensionless.

For the purpose of numerics we pose the problem not in whole space  $\mathbb{R}^3$ , but on the space-time cylinder  $\Omega_T := \Omega \times (0, T)$ , where  $\Omega := \prod_{\ell=1}^3 [0, L_\ell]$  is a rectangular cuboid, and  $T > 0$ .

We chose periodic boundary conditions on  $\Omega$  for  $u(x, t)$  and a regular initial conditions  $u(x, 0) = u^0(x)$ ,  $x \in \Omega$ , where  $u^0 \in C^\infty(\bar{\Omega})^2$  is periodic.

Imposing the Coulomb gauge, i.e., requiring that  $\nabla \cdot \mathbf{A} = 0$ , and writing individually the two equations in (3), we obtain the system

$$\begin{aligned} i\varepsilon \partial_t u_1 &= \left[ -\frac{\varepsilon^2}{2} \nabla^2 + i\varepsilon \mathbf{A} \cdot \nabla + \left( \frac{1}{2} |\mathbf{A}|^2 + \phi - \frac{\varepsilon}{2} B_3 \right) \right] u_1 + \left[ -\frac{\varepsilon}{2} B_1 + \frac{i\varepsilon}{2} B_2 \right] u_2, \\ i\varepsilon \partial_t u_2 &= \left[ -\frac{\varepsilon^2}{2} \nabla^2 + i\varepsilon \mathbf{A} \cdot \nabla + \left( \frac{1}{2} |\mathbf{A}|^2 + \phi + \frac{\varepsilon}{2} B_3 \right) \right] u_2 + \left[ -\frac{\varepsilon}{2} B_1 - \frac{i\varepsilon}{2} B_2 \right] u_1. \end{aligned} \quad (4)$$

---

<sup>2</sup>The dimensionless scaling parameter is  $\varepsilon = \frac{\hbar}{mcL_I}$  where  $L_I$  is a suitable reference length. The potentials  $\mathbf{A} \rightarrow \frac{\mathbf{A}}{A_I}$  and  $\phi \rightarrow \frac{\phi}{\phi_I}$  are scaled by the factors  $A_I = \frac{mc}{q}$  and  $\phi_I = cA_I$ .

With the operators

$$\begin{aligned}\mathcal{A} &= \frac{i\varepsilon}{2}\nabla^2, \quad \mathcal{B}_1 = -\frac{i}{\varepsilon}\left(\frac{1}{2}|\mathbf{A}|^2 + \phi - \frac{\varepsilon}{2}B_3\right), \quad \mathcal{B}_2 = -\frac{i}{\varepsilon}\left(\frac{1}{2}|\mathbf{A}|^2 + \phi + \frac{\varepsilon}{2}B_3\right), \\ \mathcal{C} &= \mathbf{A} \cdot \nabla, \quad \mathcal{D}_1 = \frac{i}{2}B_1 + \frac{1}{2}B_2, \quad \mathcal{D}_2 = \frac{i}{2}B_1 - \frac{1}{2}B_2, \\ \mathfrak{A} &= \begin{pmatrix} \mathcal{A} & 0 \\ 0 & \mathcal{A} \end{pmatrix}, \quad \mathfrak{B} = \begin{pmatrix} \mathcal{B}_1 & 0 \\ 0 & \mathcal{B}_2 \end{pmatrix}, \quad \mathfrak{C} = \begin{pmatrix} \mathcal{C} & 0 \\ 0 & \mathcal{C} \end{pmatrix}, \quad \mathfrak{D} = \begin{pmatrix} 0 & \mathcal{D}_1 \\ \mathcal{D}_2 & 0 \end{pmatrix},\end{aligned}$$

we can rewrite problem (4) as

$$\partial_t u = (\mathfrak{A} + \mathfrak{B} + \mathfrak{C} + \mathfrak{D})u. \quad (5)$$

Using the standard semigroup notation, we denote its exact solution by

$$u(x, t) = e^{(t-t')(\mathfrak{A}+\mathfrak{B}+\mathfrak{C}+\mathfrak{D})}u(x, t') \quad \text{for all } x \in \Omega \text{ and } t \geq t' \geq 0.$$

The Pauli operator is split into four contributions: the kinetic part ( $\mathfrak{A}$ ), which involves the Laplace operator, the potential part ( $\mathfrak{B}$ ), which collects the scalar terms of the potentials and the diagonal part of the spin term, the advection part ( $\mathfrak{C}$ ), which includes the convection due the magnetic vector potential, and the coupling part ( $\mathfrak{D}$ ), peculiar of the Pauli equation, which collects the off-diagonal part of the spin term and in general determines the coupling of the two components of the spinor.

In view of this decomposition, the idea is to approach the time discretization of the Pauli equation with a four-term operator splitting method in analogy with the three-term splitting method proposed in [7, 8, 9] for the scalar magnetic Schrödinger equation.

Given an integer  $N > 0$ , we consider a uniform partition of the time interval  $[0, T]$  with time-step size  $\Delta t := T/N$ , i.e.,  $t_n := n\Delta t$  for all  $n = 0, \dots, N$ , and denote by  $U^n(x)$  the numerical approximation of  $u(x, t_n)$ . We consider the Lie exponential splitting scheme

$$U^{n+1} = e^{\Delta t \mathfrak{D}} e^{\Delta t \mathfrak{C}} e^{\Delta t \mathfrak{A}} e^{\Delta t \mathfrak{B}} U^n,$$

so in the implementation, this method needs to solve each of the four steps separately to advance the state by one time-step  $\Delta t$ . Extensions of the results in this paper to higher order splitting methods such as Strang splitting are straightforward. For special cases, e.g., for time-independent potentials, significant computational cost can be saved in some of the steps by pre-computing the (then analytical) solution outside of the solution step loop for all of the intended simulation time.

For the spatial discretization of  $\Omega := \prod_{\ell=1}^3 [0, L_\ell]$ , for  $N_\ell \geq 2$  and  $\ell = 1, 2, 3$ , let  $\Delta x_\ell = L_\ell/N_\ell$ . We define the grid size as  $|\Delta x|$ , where  $\Delta x = (\Delta x_1, \Delta x_2, \Delta x_3)$ . The set of grid points  $\{x_j\}$  then consists of points  $x_j = (\frac{j_1 L_1}{N_1}, \frac{j_2 L_2}{N_2}, \frac{j_3 L_3}{N_3})$ , where  $\mathbf{j} = (j_1, j_2, j_3)$  with  $0 \leq j_\ell \leq N_\ell - 1$ . We denote the values of a periodic function  $v : \Omega \rightarrow \mathbb{C}^2$  at the grid points as

$$v_{j_1, j_2, j_3} := v(x_j) = v\left(\frac{j_1 L_1}{N_1}, \frac{j_2 L_2}{N_2}, \frac{j_3 L_3}{N_3}\right).$$

Some steps of the splitting scheme will be performed in Fourier space. To that end, for a given periodic function  $v : \Omega \rightarrow \mathbb{C}^2$ , we denote by  $\widehat{v}_{k_1, k_2, k_3}$  its discrete Fourier transform computed via FFT, i.e.,

$$\widehat{v}_{k_1, k_2, k_3} = \frac{1}{N_1 N_2 N_3} \sum_{j_1=0}^{N_1-1} \sum_{j_2=0}^{N_2-1} \sum_{j_3=0}^{N_3-1} v_{j_1, j_2, j_3} e^{-2\pi i \sum_{\ell=1}^3 \frac{j_\ell k_\ell}{N_\ell}}.$$

In the following algorithm, we summarize the structure of the proposed exponential time splitting scheme.

**Algorithm 2.1** (Lie splitting scheme for the Pauli equation). **Input.**  $U^0 \approx u^0$ .

**Loop.** For each  $n = 0, \dots, N-1$ , iterate the following steps:

- (i) *Potential step:* Compute  $U^{n*} = e^{\Delta t \mathfrak{B}} U^n$  in physical space;
- (ii) *Kinetic step:* Compute  $U^{n**} = e^{\Delta t \mathfrak{A}} U^{n*}$  in Fourier space;
- (iii) *Advection step:* Compute  $U^{n***} = e^{\Delta t \mathfrak{C}} U^{n**}$  in Fourier space;
- (iv) *Coupling step:* Compute  $U^{n+1} = e^{\Delta t \mathfrak{D}} U^{n***}$  in physical space.

**Output.**  $U^N(x_j) \approx u(x_j, t_N)$ .

In the remainder of this section, we comment on our choices for the computation of each of the four steps of Algorithm 2.1, but in principle also different solvers of consistent accuracy can be used.

### 2.1. Potential step

Step (i) of Algorithm 2.1 consists in finding, for all grid points  $x_j$ , the solution to the initial value problem

$$\begin{aligned} \partial_s \begin{pmatrix} w_{j1}(s) \\ w_{j2}(s) \end{pmatrix} &= \begin{pmatrix} \mathfrak{B}_1(s) & 0 \\ 0 & \mathfrak{B}_2(s) \end{pmatrix} \begin{pmatrix} w_{j1}(s) \\ w_{j2}(s) \end{pmatrix} \quad \text{for } s \in (0, \Delta t), \\ w_j(0) &= U^n(x_j), \end{aligned}$$

where  $w_j = (w_{j1}, w_{j2})$  and

$$\begin{aligned} \mathfrak{B}_1(s) &= -\frac{i}{\varepsilon} \left( \frac{1}{2} |\mathbf{A}(x_j, t_n + s)|^2 + \phi(x_j, t_n + s) - \frac{\varepsilon}{2} B_3(x_j, t_n + s) \right), \\ \mathfrak{B}_2(s) &= -\frac{i}{\varepsilon} \left( \frac{1}{2} |\mathbf{A}(x_j, t_n + s)|^2 + \phi(x_j, t_n + s) + \frac{\varepsilon}{2} B_3(x_j, t_n + s) \right). \end{aligned}$$

Then, the solution of the potential step is given by  $U^{n*}(x_j) = e^{\Delta t \mathfrak{B}} U^n(x_j) := w_j(\Delta t)$ . For time-independent magnetic field and potentials, an analytical solution is available for all time-steps outside of the solution loop, whereas for time-dependent data the solution has to be re-computed in each time-step. In the latter case the solution can be obtained with any highly efficient ODE solver.

## 2.2. Kinetic step

In Step (ii) of Algorithm 2.1, one has to solve the initial boundary value problem

$$\begin{aligned} \partial_t \begin{pmatrix} w_1 \\ w_2 \end{pmatrix} &= \begin{pmatrix} \frac{i\varepsilon}{2} \nabla^2 & 0 \\ 0 & \frac{i\varepsilon}{2} \nabla^2 \end{pmatrix} \begin{pmatrix} w_1 \\ w_2 \end{pmatrix} \quad \text{in } \Omega \times (t_n, t_{n+1}), \\ w(t_n) &= U^{n*}, \end{aligned}$$

which consists of nothing but two decoupled free Schrödinger equations with periodic boundary conditions for  $w = (w_1, w_2)$ . Then, the solution of the kinetic step is given by  $U^{n**} = e^{\Delta t \mathfrak{A}} U^{n*} := w(t_{n+1})$ . Hence, we can use any of the available highly efficient methods for the free Schrödinger equation. In light of the advection step, a good way is to solve the equation in Fourier space using FFT. In particular, as  $U^{n**} = e^{\Delta t \mathfrak{A}} U^{n*}$ , we find that

$$\begin{aligned} \widehat{U}_{k_1, k_2, k_3}^{n**} &= e^{-\frac{i\varepsilon\Delta t}{2} \sum_{\ell=1}^3 \left(\frac{2\pi k_\ell}{N_\ell}\right)^2} \widehat{U}_{k_1, k_2, k_3}^{n*} \\ &= e^{-\frac{i\varepsilon\Delta t}{2} \sum_{\ell=1}^3 \left(\frac{2\pi k_\ell}{N_\ell}\right)^2} \frac{1}{N_1 N_2 N_3} \sum_{j_1=0}^{N_1-1} \sum_{j_2=0}^{N_2-1} \sum_{j_3=0}^{N_3-1} U_{j_1, j_2, j_3}^{n*} e^{-2\pi i \sum_{\ell=1}^3 \frac{j_\ell k_\ell}{N_\ell}}. \end{aligned} \quad (6)$$

Then, instead of performing an iFFT to move back to physical space we can directly pass the Fourier space data to the next step.

## 2.3. Advection step

This substep is the most subtle step of the operator splitting method, as standard methods are usually stable only under restrictive CFL-type conditions that prevent the use of large time-step sizes. However, since it is analogous to the magnetic Schrödinger equation case, we can adapt methods in [7, 8, 9] for the 2-spinor case. We opt for the method of characteristics to solve this equation combined with Fourier interpolation. Step (iii) of Algorithm 2.1 consists of the solution of

$$\begin{aligned} \partial_t \begin{pmatrix} w_1 \\ w_2 \end{pmatrix} &= \begin{pmatrix} \mathbf{A} \cdot \nabla & 0 \\ 0 & \mathbf{A} \cdot \nabla \end{pmatrix} \begin{pmatrix} w_1 \\ w_2 \end{pmatrix} \quad \text{in } \Omega \times (t_n, t_{n+1}), \\ w(t_n) &= U^{n**}. \end{aligned}$$

For each of the two components of  $w = (w_1, w_2)$  and each  $\mathbf{j}$ , the characteristic  $z_{\mathbf{j}}(\cdot)$  through  $x_{\mathbf{j}}$  solves the problem

$$\partial_t z_{\mathbf{j}}(t) = -\mathbf{A}(z_{\mathbf{j}}(t), t) \quad \text{for } t \in (t_n, t_{n+1}), \quad (7)$$

$$z_{\mathbf{j}}(t_{n+1}) = x_{\mathbf{j}}. \quad (8)$$

with end value prescribed at  $t = t_{n+1}$ . Solving the above characteristic equation for each grid point  $x_{\mathbf{j}}$  would yield the sought approximation  $U^{n***}(x_{\mathbf{j}})$  via

$$U^{n***}(x_{\mathbf{j}}) = e^{\Delta t \mathfrak{C}} U^{n**}(x_{\mathbf{j}}) := w(z_{\mathbf{j}}(t_n), t_n) = U^{n**}(z_{\mathbf{j}}(t_n)).$$

However, the point  $z_j(t_n)$  is not a grid point in general, so we do not have immediate access to the value  $U^{n**}(z_j(t_n))$ . We need to use an interpolation method to approximate  $U^{n**}(z_j(t_n))$  based on the knowledge of  $U^{n**}$  at grid points. Since the previous step passes Fourier data to the advection step, it is natural to use Fourier interpolation to accomplish this. Following [8, Section 5.1], we evaluate a Fourier interpolation at  $x = z_j(t_n)$ , where the coefficients  $\{\widehat{U}_{k_1, k_2, k_3}^{n**}\}$  are known from step (ii) of Algorithm 2.1. In general, further choices are required to make such a trigonometric interpolation unique in a sensible way (see, e.g., [10]) but we omit discussion of this here - minimally oscillatory interpolations are usually to be preferred. Besides this uniform trigonometric method, one could employ other methods for the interpolation, e.g. the computationally more efficient non-uniform NUFFT-based approaches as in [8, Section 5.3] and [9, Section 2.2].

#### 2.4. Coupling step

The coupling step contains the off-diagonal components of the Pauli equation. Step (iv) of Algorithm 2.1 consists in finding, for all grid points  $x_j$ , the solution of the following initial value problem:

$$\begin{aligned} \partial_s \begin{pmatrix} w_{j1}(s) \\ w_{j2}(s) \end{pmatrix} &= \begin{pmatrix} 0 & \mathfrak{D}_1(s) \\ \mathfrak{D}_2(s) & 0 \end{pmatrix} \begin{pmatrix} w_{j1}(s) \\ w_{j2}(s) \end{pmatrix} \quad \text{for } s \in (0, \Delta t), \\ w_j(0) &= U^{n***}(x_j), \end{aligned}$$

where  $w_j = (w_{j1}, w_{j2})$  and

$$\begin{aligned} \mathfrak{D}_1(s) &= \frac{i}{2} B_1(x_j, t_n + s) + \frac{1}{2} B_2(x_j, t_n + s), \\ \mathfrak{D}_2(s) &= \frac{i}{2} B_1(x_j, t_n + s) - \frac{1}{2} B_2(x_j, t_n + s). \end{aligned}$$

Then, the solution of the coupling step, which is also the approximation  $U^{n+1} \approx u(t_{n+1})$ , is given by  $U^{n+1}(x_j) = e^{\Delta t \mathfrak{D}} U^{n***}(x_j) := w_j(\Delta t)$ . Unlike the previous steps, this is a *coupled* system of ODEs, which may be treated with appropriate highly efficient solvers. An analytic solution to this ODE is readily available in each time step, and as with the potential step (step (i) of Algorithm 2.1), for the case of time-independent potentials the solution operator may in fact be pre-computed for all considered time-steps outside of the solution loop.

**Remark 2.2.** *The potential step (i) and the coupling step (iv) can be combined into a single step if an overall reduction of the number of loop steps takes priority over other considerations, however as seen in the error analysis section, separating the coupling and potential step in this way does not incur worse stability or convergence properties.*

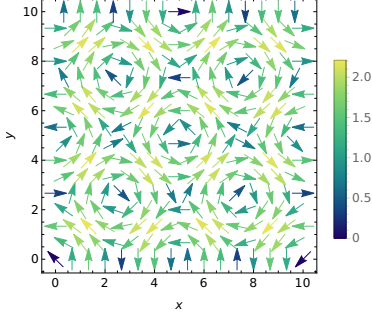


Figure 1: Visualizations of  $\mathbf{A}$  field for numerical experiments in the form of a  $x_1x_2$ -plane cross section.

### 3. Numerical experiments

Before proceeding with the analysis of the scheme we present some numerical results obtained from an implementation of the proposed method as a first order Lie splitting scheme. Significantly higher precision may be obtained than is illustrated in this section by decreasing the stepsize in space and time, as well as using a second or higher order Strang splitting but as we explore the stability and convergence properties in detail analytically in section 4.1 the purpose of this section is merely a proof of concept. The computations presented in this section have been performed with an implementation of the above method in the Julia programming language [11]. We consider two cases with different spin coupling behavior and set  $\Omega = [0, 10]^3$ ,  $\Delta x = 0.4$  and  $\varepsilon = 0.5$  for both numerical experiments.

#### 3.1. Decoupled spin state dynamics

We seek numerical solutions of the Pauli equation (1) using the following constant-in-time fields, which are periodic on  $\Omega$ :

$$\mathbf{A}(x) = \pi \begin{pmatrix} -\cos\left(\frac{\pi}{5}(x_2 - 5)\right) \sin\left(\frac{\pi}{5}(x_2 - 5)\right) \\ \cos\left(\frac{\pi}{5}(x_1 - 5)\right) \sin\left(\frac{\pi}{5}(x_1 - 5)\right) \\ 0 \end{pmatrix}, \quad (9)$$

$$\mathbf{B}(x) = \frac{\pi}{5} \begin{pmatrix} 0 \\ 0 \\ \sum_{j=1}^2 \left( \pi \cos\left(\frac{\pi}{5}(x_j - 5)\right)^2 - \pi \sin\left(\frac{\pi}{5}(x_j - 5)\right)^2 \right) \end{pmatrix}, \quad (10)$$

$$\phi(x) = 0. \quad (11)$$

It is easily confirmed that these fields satisfy  $\mathbf{B} = \nabla \times \mathbf{A}$  as well as the Coulomb gauge  $\nabla \cdot \mathbf{A} = 0$ . Due to absent  $x_3$ -component in the vector potential, one can visualize it concisely in a 2-dimensional  $x_1x_2$ -plane cut vector plot as depicted in Figure 1. Figure 2 shows the absolute value of the solution obtained for the

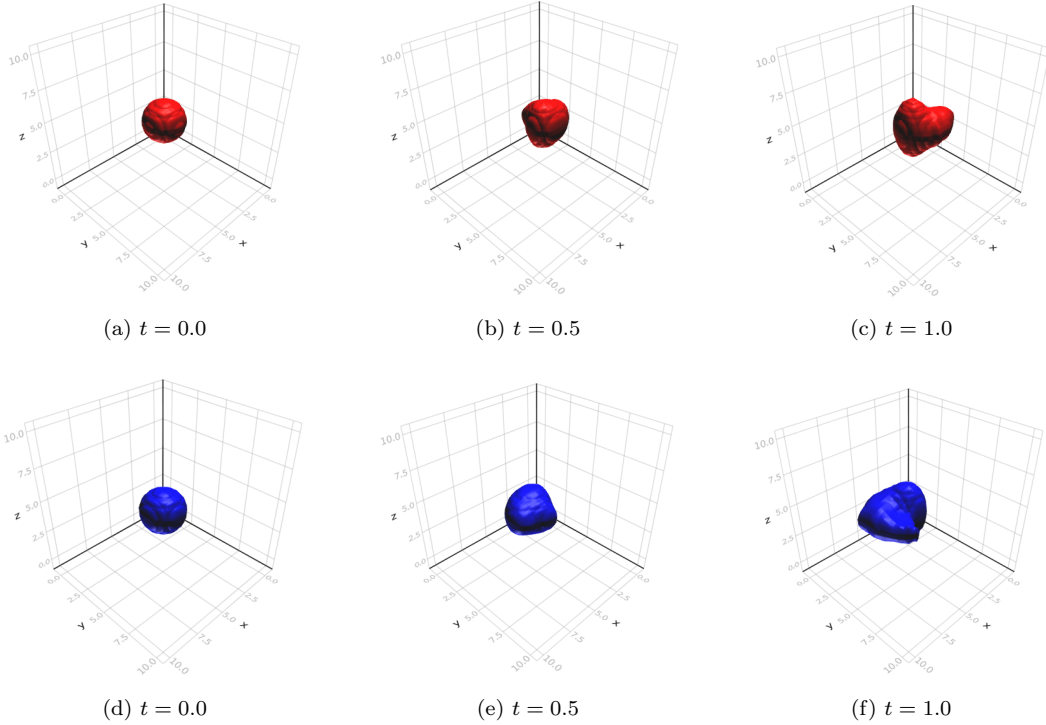


Figure 2: Isosurfaces of constant value 0.055 for fields in (9) and initial state in (12). Absolute value of spin up component displayed in red and absolute value of spin down component in blue. The two spin components evolve independently.

initial state

$$u^0 = \begin{pmatrix} e^{-(x_1-4.5)^2-(x_2-4.5)^2-(x_3-5)^2} \\ e^{-(x_1-5.5)^2-(x_2-5.5)^2-(x_3-5)^2} \end{pmatrix}, \quad (12)$$

at different times visualized as isosurfaces. As the  $\mathbf{B}$  field lacks an  $x$ -component, there is no coupling between spin up and down components and the spin components evolve fully independently indefinitely. In the absence of analytic solutions we can compare the solutions computed with  $\Delta t = 0.05$  with more coarse time discretizations to approximately visualize the method's convergence properties. Figure 3 shows the maximal absolute and relative errors compared to the  $\Delta t = 0.05$  precision numerical approximation with respect to different time discretizations. Convergence to the approximation is at least linear as expected of a first order Lie splitting approach. If desired, an implementation of a higher order Strang splitting could be used to achieve higher orders of convergence in time, cf. [12]. We derive convergence error bounds in section 4.1.

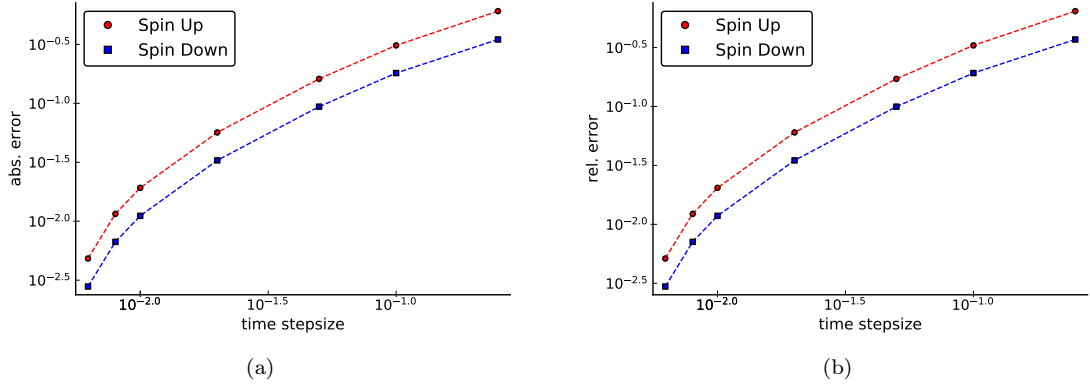


Figure 3: Absolute and relative errors of different time discretizations for the decoupled spin dynamics numerical experiment compared to a higher precision  $\Delta t = 0.05$  solution. We observe approximately linear error convergence in time, as expected from a first order Lie splitting method.

### 3.2. Coupled spin state dynamics

We use the following modified version of the above field setup to observe more complex Pauli equation phenomena:

$$\mathbf{A}(x) = \pi \begin{pmatrix} -\cos\left(\frac{\pi}{5}(x_2 - 5)\right) \sin\left(\frac{\pi}{5}(x_2 - 5)\right) \\ \cos\left(\frac{\pi}{5}(x_1 - 5)\right) \sin\left(\frac{\pi}{5}(x_1 - 5)\right) \\ \frac{1}{\pi} \cos\left(\frac{\pi}{5}(x_1 - 5)\right) \sin\left(\frac{\pi}{5}(x_2 - 5)\right) \end{pmatrix}, \quad (13)$$

$$\mathbf{B}(x) = \frac{\pi}{5} \begin{pmatrix} \cos\left(\frac{\pi}{5}(x_1 - 5)\right) \cos\left(\frac{\pi}{5}(x_2 - 5)\right) \\ \sin\left(\frac{\pi}{5}(x_1 - 5)\right) \sin\left(\frac{\pi}{5}(x_2 - 5)\right) \\ \sum_{j=1}^2 \left( \pi \cos\left(\frac{\pi}{5}(x_j - 5)\right)^2 - \pi \sin\left(\frac{\pi}{5}(x_j - 5)\right)^2 \right) \end{pmatrix}, \quad (14)$$

$$\phi(x) = 0. \quad (15)$$

In order to visualize the spin coupling phenomenon which is a core characteristic of the Pauli equation, we initialize with an exclusively spin up state:

$$u^0 = \begin{pmatrix} e^{-(x_1 - 4.5)^2 - (x_2 - 4.5)^2 - (x_3 - 5)^2} \\ 0 \end{pmatrix}. \quad (16)$$

Figure 4 shows the absolute value of the solution obtained for the initial state (16) at different times visualized as isosurfaces. Due to the presence of a non-zero  $x_1$ -component in the  $\mathbf{B}$  field, one observes coupling between spin up and down components. Figure 5 shows absolute and relative errors compared to a  $\Delta t = 0.05$  numerical approximation with respect to time discretization.

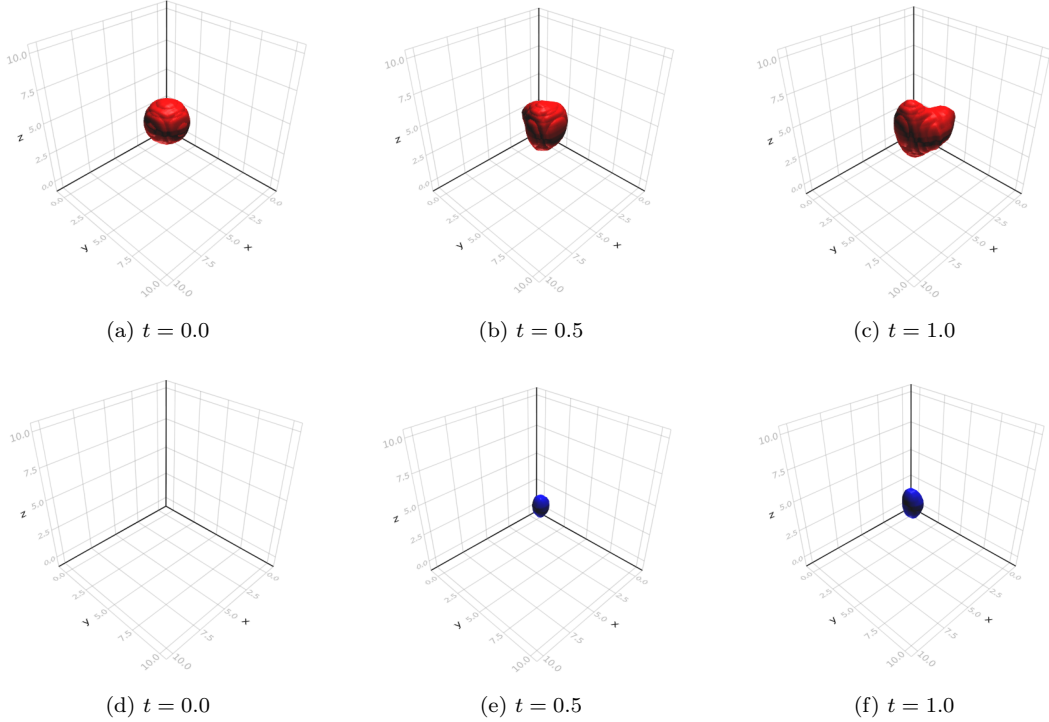


Figure 4: Isosurfaces of constant value 0.055 for fields in (13) and initial state in (16). Absolute value of spin up component displayed in red and absolute value of spin down component in blue. Notice coupling behavior of spin up and spin down components - the spin up component gradually induces a spin down component in the same location and vice versa. The coupling is bidirectional.

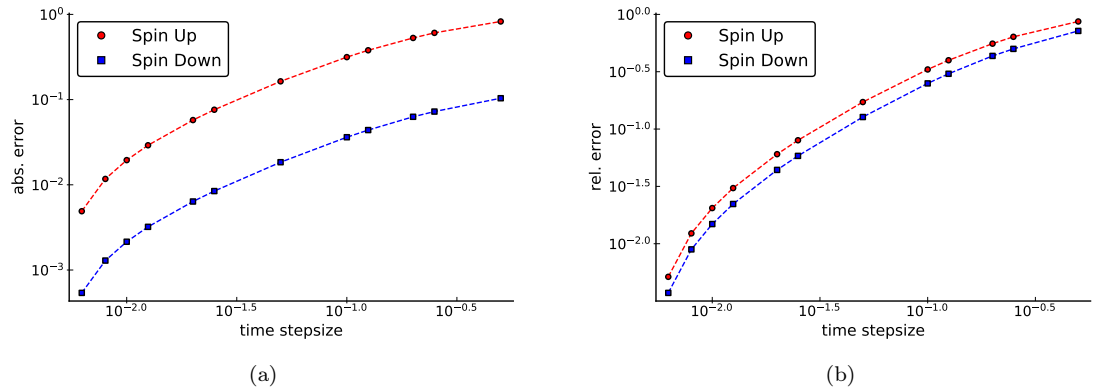


Figure 5: Absolute and relative errors of different time discretizations for the coupled spin system numerical experiment compared to a  $\Delta t = 0.05$  solution. We again observe approximately linear error convergence in time, as expected from a first order Lie splitting method.

## 4. Analysis of the method

In this section, we study the stability and the convergence of the splitting scheme described in Section 2. Our analysis largely follows the approach of [13, 7, 9]. In [8], the analysis for the proposed three-term splitting scheme for the magnetic Schrödinger equation is based on an abstract result for general three-term Lie exponential splitting methods. There, the basic idea is to bound the errors in terms of suitable bounds for the commutators [14]. Such an approach, however, does not give control of the  $\varepsilon$ -dependencies of the involved constants. Note that in this work we do not consider the semi-classical regime, cf. [15], which will be the subject of follow-up work.

### 4.1. Stability analysis

We begin by studying the stability of the scheme. Consider the discrete  $\ell^2$  norm and the  $L^2$  norm for functions given by:

$$\begin{aligned}\|\mathbf{U}_i\|_{\ell^2}^2 &= \left( \prod_{\ell=1}^3 \frac{L_\ell}{N_\ell} \right) \sum_{j_1=0}^{N_1-1} \sum_{j_2=0}^{N_2-1} \sum_{j_3=0}^{N_3-1} |U_i(x_j)|^2, \\ \|U_i\|_{L^2}^2 &= \int_{\Omega} |U_i(x)|^2 dx,\end{aligned}$$

where  $\mathbf{U}_i$  denotes the vector of coefficients  $U_i(x_j) = U_i\left(\frac{j_1 L_1}{N_1}, \frac{j_2 L_2}{N_2}, \frac{j_3 L_3}{N_3}\right)$ . The  $i$  index is added here to denote that these norms are defined for spinor components as opposed to the 2-spinor itself. The total 2-spinor norm in question is the sum of the two spinor component norms. For the sake of simplicity we assume the potentials (and hence also the magnetic field) to be time-independent, so that analytic solutions for the potential and the coupling steps are available for all time.

The following lemma then establishes the stability of the potential and kinetic steps.

**Lemma 4.1.** *Let  $U_i^{n**}(x_j)$  denote the elements of the grid point vector  $\mathbf{U}_i^{n**}$  after solving the kinetic and potential step starting from  $\mathbf{U}_i^n$ . Then, it holds that*

$$\|\mathbf{U}_i^{n**}\|_{\ell^2} = \|\mathbf{U}_i^n\|_{\ell^2}.$$

and thus

$$\|\mathbf{U}_1^{n**}\|_{\ell^2} + \|\mathbf{U}_2^{n**}\|_{\ell^2} = \|\mathbf{U}_1^n\|_{\ell^2} + \|\mathbf{U}_2^n\|_{\ell^2}.$$

*Proof.* The proof is a higher dimensional analogue of [13, Lemma 3.1]. We explicitly omit the  $i$ -index notation above in this proof despite the functions being spinor *components* as opposed to the full 2-spinor to avoid

excessive notational clutter. It holds that

$$\begin{aligned}
\|\mathbf{U}^{n***}\|_{\ell^2}^2 &= \left( \prod_{\ell=1}^3 \frac{L_\ell}{N_\ell} \right) \sum_{\mathbf{j}} |U^{n**}(x_{\mathbf{j}})|^2 = \left( \prod_{\ell=1}^3 \frac{L_\ell}{N_\ell^2} \right) \sum_{\mathbf{k}} |\widehat{U}_{k_1, k_2, k_3}^{n**}|^2 \\
&= \left( \prod_{\ell=1}^3 \frac{L_\ell}{N_\ell^2} \right) \sum_{\mathbf{k}} |e^{-\frac{i\varepsilon\Delta t}{2} \sum_{\ell=1}^3 \left(\frac{2\pi k_\ell}{L_\ell}\right)^2} \widehat{U}_{k_1, k_2, k_3}^{n*}|^2 = \left( \prod_{\ell=1}^3 \frac{L_\ell}{N_\ell^2} \right) \sum_{\mathbf{k}} |\widehat{U}_{k_1, k_2, k_3}^{n*}|^2 \\
&= \left( \prod_{\ell=1}^3 \frac{L_\ell}{N_\ell} \right) \sum_{\mathbf{j}} |U^{n*}(x_{\mathbf{j}})|^2 = \|\mathbf{U}^{n*}\|_{\ell^2}^2,
\end{aligned}$$

where we used the shorthands

$$\sum_{\mathbf{j}} \rightarrow \sum_{j_1=0}^{N_1-1} \sum_{j_2=0}^{N_2-1} \sum_{j_3=0}^{N_3-1} \quad \text{and} \quad \sum_{\mathbf{k}} \rightarrow \sum_{k_1=0}^{N_1-1} \sum_{k_2=0}^{N_2-1} \sum_{k_3=0}^{N_3-1}.$$

The second and fifth step of the above computation make use of a higher dimensional variant of Plancherel's theorem (compare, e.g., [16]) which exploits a generalization of the same structure used for the one-dimensional Schrödinger variant in [13]. The potential step can be solved exactly and, in the case of time-independent potentials, also for all time, so the remaining statement  $\|\mathbf{U}^{n*}\|_{\ell^2}^2 = \|\mathbf{U}^n\|_{\ell^2}^2$  is straightforward. The summation of both spinor component results is obvious and completes the proof.  $\square$

As the advection step does not structurally change from the magnetic Schrödinger equation, a similar result for the advection step is a corollary of previous results.

**Lemma 4.2.** *Under the assumption that errors from the interpolation and backwards step are negligible and  $\nabla \cdot \mathbf{A} = 0$ , the advection step solution satisfies*

$$\|U_{I,i}^{n***}\|_{L^2} \leq \|U_{I,i}^{n**}\|_{L^2},$$

where  $U_{I,i}^{n***}$  denotes the Fourier interpolation of the  $i$ -th spinor component  $U_i^{n***}$ , and thus

$$\|U_{I,1}^{n***}\|_{L^2} + \|U_{I,2}^{n***}\|_{L^2} \leq \|U_{I,1}^{n**}\|_{L^2} + \|U_{I,2}^{n***}\|_{L^2}.$$

*Proof.* See proofs of analogous results in [9, Lemma 3.2] and [17, Theorem 1] for the first statement. The second is an immediate corollary.  $\square$

**Lemma 4.3.** *Let  $\mathbf{U}_i^{n+1}$  denote the grid point vector after solving the coupling step starting from  $\mathbf{U}_i^{n***}$ . Then, it holds that*

$$\|\mathbf{U}_1^{n+1}\|_{\ell^2} + \|\mathbf{U}_2^{n+1}\|_{\ell^2} = \|\mathbf{U}_1^{n***}\|_{\ell^2} + \|\mathbf{U}_2^{n***}\|_{\ell^2}.$$

*Proof.* The coupling step may be solved analytically as with the potential step before and thus any analysis of this sort can be reduced to an analysis of this exact solution. However, for the coupling step unlike for the potential step, the namesake coupling of spin states must be considered, as it allows for ‘mass’ or ‘charge’

exchange. While the solution operator  $e^{\Delta t \mathcal{D}}$  is unitary, unlike in the other cases the spinor-component-wise operators are not necessarily unitary. This implies that while

$$\|\mathbf{U}_1^{n+1}\|_{\ell^2} + \|\mathbf{U}_2^{n+1}\|_{\ell^2} = \|\mathbf{U}_1^{n***}\|_{\ell^2} + \|\mathbf{U}_2^{n***}\|_{\ell^2}.$$

still holds by canonical proofs of unitarity of such an operator as well as conservation of mass in the Pauli equation, mass conservation in the single components is not generally true.  $\square$

**Remark 4.4.** *Unlike for the kinetic, advection and potential steps, the above result only holds for the total norm of the 2-spinor and not for the individual components. This is not an artifact of the method but an effect of the physics, as spin up and spin down states generally couple in the presence of magnetic fields.*

In the following theorem, we establish the stability of Algorithm 2.1.

**Theorem 4.5.** *Let  $\mathbf{U}^{n+1}$  be the grid point vector after passing through all of the steps outlined in Algorithm 2.1 once, starting from  $\mathbf{U}^n$ . Then, it holds that*

$$\|\mathbf{U}_1^{n+1}\|_{\ell^2} + \|\mathbf{U}_2^{n+1}\|_{\ell^2} \leq \|\mathbf{U}_1^n\|_{\ell^2} + \|\mathbf{U}_2^n\|_{\ell^2}.$$

*Proof.* Applying Lemma 4.1 and 4.2 sequentially we see that

$$\|\mathbf{U}_i^{n***}\|_{\ell^2} = \|U_{I,i}^{n***}\|_{L^2} \leq \|U_{I,i}^{n**}\|_{L^2} = \|\mathbf{U}_i^{n**}\|_{\ell^2} = \|\mathbf{U}_i^n\|_{\ell^2},$$

and thus

$$\|\mathbf{U}_1^{n***}\|_{\ell^2} + \|\mathbf{U}_2^{n***}\|_{\ell^2} \leq \|\mathbf{U}_1^n\|_{\ell^2} + \|\mathbf{U}_2^n\|_{\ell^2}.$$

The conclusion then follows via Lemma 4.3.  $\square$

#### 4.2. Error estimates

In this section we study error estimates for the proposed method. For this purpose we will make use of the following shorthands to avoid overly long and repeated summation notation:

$$\|\mathbf{U}\|_{\alpha} = \|\mathbf{U}_1\|_{\ell^2} + \|\mathbf{U}_2\|_{\ell^2},$$

$$\|u\|_A = \|u_1\|_{L^2} + \|u_2\|_{L^2}.$$

The main result of this section will be using the following assumptions, which are analogues of the assumptions for the scalar Schrödinger-type equation in [13, 7, 9]: For all  $m \geq 1$  let

$$\left\| \frac{\partial^{m_1}}{\partial x^{m_1}} \frac{\partial^{m_2}}{\partial t^{m_2}} u_i(x, t) \right\|_{L^2} \leq \frac{\alpha_{m_1+m_2}}{\varepsilon^{m_1+m_2}}, \quad (17)$$

$$\left\| \frac{\partial^m}{\partial x^m} \mathbf{A}(x) \right\|_{L^2} \leq \beta_m, \quad (18)$$

$$\left\| \frac{\partial^m}{\partial x^m} \phi(x) \right\|_{L^2} \leq \gamma_m, \quad (19)$$

where  $m, m_1, m_2 \in \mathbb{N}$ , while  $\alpha_m, \beta_m$  and  $\gamma_m$  are constants and  $\varepsilon$  is the (small) scaling parameter appearing in the scaled Pauli equation. Wherever we write  $u_i$  without specific index  $i$  we mean to imply that the statement holds for both of the 2-spinor components individually and thus has an obvious extension to the  $\alpha$  and  $A$  norms defined above.

**Theorem 4.6.** *Denote the exact 2-spinor solution to the Pauli equation in (5) for given parameter  $\varepsilon$  by*

$$u^\varepsilon(x, t) = \begin{pmatrix} u_1^\varepsilon(x, t) \\ u_2^\varepsilon(x, t) \end{pmatrix}, \text{ where}$$

$$u^\varepsilon(x, t + \Delta t) = e^{\Delta t \mathfrak{A} + \Delta t \mathfrak{B} + \Delta t \mathfrak{C} + \Delta t \mathfrak{D}} u^\varepsilon(x, t),$$

and its operator splitting numerical approximation at time  $n\Delta t$  by  $U^n$ , where

$$U^{n+1} = e^{\Delta t \mathfrak{D}} e^{\Delta t \mathfrak{C}} e^{\Delta t \mathfrak{A}} e^{\Delta t \mathfrak{B}} U^n.$$

We assume that the potentials and solution are smooth and periodic on the relevant spatial box, that the characteristic equation in (7) in the advection step and the FFT steps may be solved with negligible error along with the assumption statements listed in (17)–(19) and that  $|\Delta x| = O(\varepsilon)$  and  $\Delta t = O(\varepsilon)$ . Then, for any time  $t \in [0, T]$  and for some  $m \in \mathbb{N}$ , we have the estimate

$$\|u^\varepsilon(t_n) - U_I^n\|_A \leq \frac{C_1 T}{\Delta t} \left( \frac{|\Delta x|}{\varepsilon} \right)^m + \frac{C_2 T \Delta t}{\varepsilon},$$

with  $C_1, C_2$  being constants independent of  $\Delta t$ ,  $\Delta x$ ,  $T$ , and  $\varepsilon$ .

*Proof.* Similar to discussions in [13, Theorem 4.1], [7, Theorem 4] and [9, Theorem 3.2] for various cases of scalar Schrödinger-type equations, the local splitting error for the Pauli equation operator splitting method is also determined by the non-commutativity of the respective operators via the classical Baker–Campbell–Hausdorff formula. The proof strategy thus begins with the computation of commutators  $[\cdot, \cdot]$  for the operators  $\Delta t \mathfrak{A}$ ,  $\Delta t \mathfrak{B}$ ,  $\Delta t \mathfrak{C}$  and  $\Delta t \mathfrak{D}$  and then concludes via a triangle inequality estimation for the error and can thus be seen as a 2-spinor generalization of the above referenced theorems. The errors in the 2-spinor components are coupled via the coupling step operator, thus the final result on the error is a result for the combined error in both components as opposed to a component-wise error.

As the operators in question act on 2-spinors and have a block operator representation we make use of the observation that the commutators of such operators  $\mathfrak{L}, \mathfrak{M}, \mathfrak{K}$  with form

$$\mathfrak{L} = \begin{pmatrix} L & 0 \\ 0 & L \end{pmatrix}, \quad \mathfrak{M} = \begin{pmatrix} M_1 & 0 \\ 0 & M_2 \end{pmatrix}, \quad \mathfrak{K} = \begin{pmatrix} 0 & K_1 \\ K_2 & 0 \end{pmatrix}$$

satisfy

$$\begin{aligned}
[\mathfrak{L}, \mathfrak{M}] &= \begin{pmatrix} [L, M_1] & 0 \\ 0 & [L, M_2] \end{pmatrix}, \\
[\mathfrak{M}, \mathfrak{K}] &= \begin{pmatrix} 0 & M_1 K_1 - K_1 M_2 \\ M_2 K_2 - K_2 M_1 & 0 \end{pmatrix}, \\
[\mathfrak{L}, \mathfrak{K}] &= \begin{pmatrix} 0 & [L, K_1] \\ [L, K_2] & 0 \end{pmatrix}.
\end{aligned}$$

The computation can thus be made easier by computing these for each of the relevant component operators of  $\Delta t \mathfrak{A}$ ,  $\Delta t \mathfrak{B}$ ,  $\Delta t \mathfrak{C}$  and  $\Delta t \mathfrak{D}$ , which we re-list here for convenience:

$$\begin{aligned}
\mathcal{A} &= \frac{i\varepsilon}{2} \nabla^2, \quad \mathcal{B}_1 = -\frac{i}{\varepsilon} \left( \frac{1}{2} |\mathbf{A}|^2 + \phi - \frac{\varepsilon}{2} B_3 \right), \quad \mathcal{B}_2 = -\frac{i}{\varepsilon} \left( \frac{1}{2} |\mathbf{A}|^2 + \phi + \frac{\varepsilon}{2} B_3 \right), \\
\mathcal{C} &= \mathbf{A} \cdot \nabla, \quad \mathcal{D}_1 = \frac{i}{2} B_1 + \frac{1}{2} B_2, \quad \mathcal{D}_2 = \frac{i}{2} B_1 - \frac{1}{2} B_2.
\end{aligned}$$

Direct computation yields the following results for the commutators of  $\mathcal{A}$ ,  $\mathcal{B}$  and  $\mathcal{C}$ :

$$\begin{aligned}
[\Delta t \mathcal{A}, \Delta t \mathcal{B}_1] u_1 &= \frac{(\Delta t)^2}{2} \sum_{j=1}^3 \partial_j^2 \left( \frac{1}{2} |\mathbf{A}|^2 + \phi - \frac{\varepsilon}{2} B_3 \right) u_1 \\
&\quad + (\Delta t)^2 \sum_{j=1}^3 \partial_j \left( \frac{1}{2} |\mathbf{A}|^2 + \phi - \frac{\varepsilon}{2} B_3 \right) \partial_j u_1, \\
[\Delta t \mathcal{A}, \Delta t \mathcal{B}_2] u_2 &= \frac{(\Delta t)^2}{2} \sum_{j=1}^3 \partial_j^2 \left( \frac{1}{2} |\mathbf{A}|^2 + \phi + \frac{\varepsilon}{2} B_3 \right) u_2 \\
&\quad + (\Delta t)^2 \sum_{j=1}^3 \partial_j \left( \frac{1}{2} |\mathbf{A}|^2 + \phi + \frac{\varepsilon}{2} B_3 \right) \partial_j u_2, \\
[\Delta t \mathcal{A}, \Delta t \mathcal{C}] u_i &= \frac{i\varepsilon(\Delta t)^2}{2} \sum_{k=1}^3 \sum_{j=1}^3 (\partial_k^2 A_j \partial_j u_i + 2\partial_k A_j \partial_k \partial_j u_i), \\
[\Delta t \mathcal{C}, \Delta t \mathcal{B}_1] u_1 &= -\frac{i(\Delta t)^2}{\varepsilon} \sum_{j=1}^3 A_j \partial_j \left( \frac{1}{2} |\mathbf{A}|^2 + \phi - \frac{\varepsilon}{2} B_3 \right) u_1, \\
[\Delta t \mathcal{C}, \Delta t \mathcal{B}_2] u_2 &= -\frac{i(\Delta t)^2}{\varepsilon} \sum_{j=1}^3 A_j \partial_j \left( \frac{1}{2} |\mathbf{A}|^2 + \phi + \frac{\varepsilon}{2} B_3 \right) u_2.
\end{aligned}$$

This covers the operators which are already present in the magnetic Schrödinger case. The primary takeaway from this is that, under assumptions (17)–(19), all of these commutators are of order  $O\left(\frac{(\Delta t)^2}{\varepsilon}\right)$ , since all the terms involving  $O\left(\frac{(\Delta t)^2}{\varepsilon^2}\right)$  cancel, which is consistent with the fact that this method is a Pauli equation generalization of methods described in [13, 7, 9]. This even holds true for the  $\mathfrak{B}$  operator which differs from the magnetic Schrödinger case by a term involving the magnetic field, i.e., the curl of the vector potential. Finally the coupling step must be examined carefully, as it introduces an additional element to the local

splitting error. Direct computation of the components of the coupling step commutators yields:

$$\begin{aligned}
[\Delta t \mathcal{A}, \Delta t \mathcal{D}_1] u_2 &= \frac{(\Delta t)^2}{2} \sum_{j=1}^3 \partial_j^2 \left( -\frac{\varepsilon}{2} B_1 + \frac{i\varepsilon}{2} B_2 \right) u_1 \\
&\quad + (\Delta t)^2 \sum_{j=1}^3 \partial_j \left( -\frac{\varepsilon}{2} B_1 + \frac{i\varepsilon}{2} B_2 \right) \partial_j u_2, \\
[\Delta t \mathcal{A}, \Delta t \mathcal{D}_2] u_1 &= \frac{(\Delta t)^2}{2} \sum_{j=1}^3 \partial_j^2 \left( -\frac{\varepsilon}{2} B_1 - \frac{i\varepsilon}{2} B_2 \right) u_1 \\
&\quad + (\Delta t)^2 \sum_{j=1}^3 \partial_j \left( -\frac{\varepsilon}{2} B_1 - \frac{i\varepsilon}{2} B_2 \right) \partial_j u_1, \\
[\Delta t \mathcal{C}, \Delta t \mathcal{D}_1] u_2 &= (\Delta t)^2 \sum_{j=1}^3 A_j \partial_j \left( \frac{i}{2} B_1 + \frac{1}{2} B_2 \right) u_2, \\
[\Delta t \mathcal{C}, \Delta t \mathcal{D}_2] u_1 &= (\Delta t)^2 \sum_{j=1}^3 A_j \partial_j \left( \frac{i}{2} B_1 - \frac{1}{2} B_2 \right) u_1, \\
\Delta t^2 (\mathcal{B}_1 \mathcal{D}_1 - \mathcal{D}_1 \mathcal{B}_2) u_2 &= \frac{(\Delta t)^2}{2} (-B_1 B_3 + i B_2 B_3), \\
\Delta t^2 (\mathcal{B}_2 \mathcal{D}_2 - \mathcal{D}_2 \mathcal{B}_1) u_1 &= \frac{(\Delta t)^2}{2} (B_1 B_3 + i B_2 B_3).
\end{aligned}$$

Under assumptions (17)–(19) all of these terms are  $O((\Delta t)^2)$ . As  $\Delta t = O(\varepsilon)$  this means the coupling step commutators contribute less to the error than the remaining operators. Combining these results for all of the commutators, one finds that the local splitting error is at worst of order

$$\|u^\varepsilon(t_{n+1}) - \tilde{u}(t_{n+1})\|_A = O\left(\frac{\Delta t^2}{\varepsilon}\right),$$

where  $\tilde{u}(t_{n+1})$  is the pre-discretization operator splitting solution satisfying

$$\tilde{u}(t_{n+1}) = e^{\Delta t \mathfrak{D}} e^{\Delta t \mathfrak{C}} e^{\Delta t \mathfrak{A}} e^{\Delta t \mathfrak{B}} u(t_n).$$

Due to the nature of the coupling step, the errors in the two spin components are not in general separable. We proceed via the triangle inequality as follows:

$$\begin{aligned}
\|u^\varepsilon(t_{n+1}) - U_I^{n+1}\|_A &\leq \|u^\varepsilon(t_{n+1}) - \tilde{u}(t_{n+1})\|_A + \|\tilde{u}(t_{n+1}) - \tilde{u}_I(t_{n+1})\|_A \\
&\quad + \|\tilde{u}_I(t_{n+1}) - U_I^{n+1}\|_A.
\end{aligned}$$

The first term on the right hand side was already shown above to be of order  $O\left(\frac{\Delta t^2}{\varepsilon}\right)$ , while the second term is nothing but the error of our interpolation method which as discussed in [7] and [18, Theorem 3] is  $O\left(\left(\frac{|\Delta x|}{\varepsilon}\right)^m\right)$ , where  $m$  is a positive integer. The final term in need of investigation is thus  $\|\tilde{u}(t_{n+1}) - U_I^{n+1}\|_A$  which corresponds to the error incurred due to the discretization. Noting that  $\|f_I\|_{L^2} = \|\mathbf{f}\|_{\ell^2}$ , we obtain

$$\begin{aligned}
\|\tilde{u}_I(t_{n+1}) - U_I^{n+1}\|_A &= \|\tilde{\mathbf{u}}(t_{n+1}) - \mathbf{U}^{n+1}\|_\alpha \\
&= \|e^{\Delta t \mathfrak{D}} e^{\Delta t \mathfrak{C}} e^{\Delta t \mathfrak{A}} e^{\Delta t \mathfrak{B}} \mathbf{u}(t_n) - e^{\Delta t \mathfrak{D}} e^{\Delta t \mathfrak{C}_N} e^{\Delta t \mathfrak{A}_N} e^{\Delta t \mathfrak{B}} \mathbf{U}^n\|_\alpha,
\end{aligned}$$

where  $\tilde{\mathbf{u}}$  and  $\mathbf{u}$  denote the vectors collecting the gridpoint values of  $\tilde{u}$  and  $u$ , respectively. As the potential and coupling steps are solved analytically the operators remain unaffected on the right hand side but for the kinetic and advection steps we must distinguish their numerical approximations  $\mathfrak{A}_N$  and  $\mathfrak{C}_N$ . A further application of the triangle inequality yields

$$\begin{aligned}\|\tilde{u}_I(t_{n+1}) - U_I^{n+1}\|_A &\leq \|e^{\Delta t \mathfrak{D}} e^{\Delta t \mathfrak{C}} e^{\Delta t \mathfrak{A}} e^{\Delta t \mathfrak{B}} \mathbf{u}(t_n) - e^{\Delta t \mathfrak{D}} e^{\Delta t \mathfrak{C}} e^{\Delta t \mathfrak{A}_N} e^{\Delta t \mathfrak{B}} \mathbf{u}(t_n)\|_\alpha \\ &\quad + \|e^{\Delta t \mathfrak{D}} e^{\Delta t \mathfrak{C}} e^{\Delta t \mathfrak{A}_N} e^{\Delta t \mathfrak{B}} \mathbf{u}(t_n) - e^{\Delta t \mathfrak{D}} e^{\Delta t \mathfrak{C}_N} e^{\Delta t \mathfrak{A}_N} e^{\Delta t \mathfrak{B}} \mathbf{u}(t_n)\|_\alpha \\ &\quad + \|e^{\Delta t \mathfrak{D}} e^{\Delta t \mathfrak{C}_N} e^{\Delta t \mathfrak{A}_N} e^{\Delta t \mathfrak{B}} \mathbf{u}(t_n) - e^{\Delta t \mathfrak{D}} e^{\Delta t \mathfrak{C}_N} e^{\Delta t \mathfrak{A}_N} e^{\Delta t \mathfrak{B}} \mathbf{U}^n\|_\alpha.\end{aligned}$$

The first term

$$\|e^{\Delta t \mathfrak{D}} e^{\Delta t \mathfrak{C}} e^{\Delta t \mathfrak{A}} e^{\Delta t \mathfrak{B}} \mathbf{u}(t_n) - e^{\Delta t \mathfrak{D}} e^{\Delta t \mathfrak{C}} e^{\Delta t \mathfrak{A}_N} e^{\Delta t \mathfrak{B}} \mathbf{u}(t_n)\|_\alpha$$

is just a measure of the spectral approximation error again and is thus  $O\left(\left(\frac{|\Delta x|}{\varepsilon}\right)^m\right)$  as described above.

The same is true for the second term

$$\|e^{\Delta t \mathfrak{D}} e^{\Delta t \mathfrak{C}} e^{\Delta t \mathfrak{A}_N} e^{\Delta t \mathfrak{B}} \mathbf{u}(t_n) - e^{\Delta t \mathfrak{D}} e^{\Delta t \mathfrak{C}_N} e^{\Delta t \mathfrak{A}_N} e^{\Delta t \mathfrak{B}} \mathbf{u}(t_n)\|_\alpha,$$

because if errors due to the computation of the backwards grid step are negligible then this step is just a measure for the interpolation accuracy and thus also  $O\left(\left(\frac{|\Delta x|}{\varepsilon}\right)^m\right)$ . The final term in question is thus

$$\|e^{\Delta t \mathfrak{D}} e^{\Delta t \mathfrak{C}_N} e^{\Delta t \mathfrak{A}_N} e^{\Delta t \mathfrak{B}} \mathbf{u}(t_n) - e^{\Delta t \mathfrak{D}} e^{\Delta t \mathfrak{C}_N} e^{\Delta t \mathfrak{A}_N} e^{\Delta t \mathfrak{B}} \mathbf{U}^n\|_\alpha.$$

Straightforward computation shows that the operators  $e^{\Delta t \mathfrak{D}}$ ,  $e^{\Delta t \mathfrak{C}}$ ,  $e^{\Delta t \mathfrak{A}}$  and  $e^{\Delta t \mathfrak{B}}$  are all unitary and thus the Lemmas leading up to Theorem 4.5 in particular also imply that

$$\|e^{\Delta t \mathfrak{C}_N}\|_A \leq 1, \quad \|e^{\Delta t \mathfrak{A}_N}\|_A = 1.$$

Using the above chain of operator norm estimates and using the stability results above, cf. [9, equation (3.50)], yields

$$\|e^{\Delta t \mathfrak{D}} e^{\Delta t \mathfrak{C}_N} e^{\Delta t \mathfrak{A}_N} e^{\Delta t \mathfrak{B}} \mathbf{u}(t_n) - e^{\Delta t \mathfrak{D}} e^{\Delta t \mathfrak{C}_N} e^{\Delta t \mathfrak{A}_N} e^{\Delta t \mathfrak{B}} \mathbf{U}^n\|_\alpha \leq \|u^\varepsilon(t_n) - U_I^n\|_A.$$

Analogous to [9, equation (3.52)] this yields the recursive relationship

$$\|u^\varepsilon(t_{n+1}) - U_I^{n+1}\|_A \leq \|u^\varepsilon(t_n) - U_I^n\|_A + O\left(\left(\frac{|\Delta x|}{\varepsilon}\right)^m\right) + O\left(\frac{\Delta t^2}{\varepsilon}\right).$$

which on the solution interval  $t \in [0, T]$  implies that

$$\|u^\varepsilon(t_n) - U_I^n\|_A \leq \frac{C_1 T}{\Delta t} \left(\frac{|\Delta x|}{\varepsilon}\right)^m + \frac{C_2 T \Delta t}{\varepsilon},$$

for some constants  $C_1$  and  $C_2$  independent of  $\Delta t$ ,  $\Delta x$ ,  $T$ , and  $\varepsilon$ .  $\square$

The above theorem is fully consistent with the view of the Pauli equation as a bottom-up generalization of the scalar magnetic Schrödinger equation as it yields analogous error bounds despite the inclusions of the coupling step as well as its inherent three-dimensional nature. Furthermore we can use the above result to define a meshing strategy for a desired accuracy (as done in [9] and [7]): If  $\delta > 0$  is a desired error bound so that  $\|u^\varepsilon(t_n) - U_I^{\varepsilon,n}\|_\beta \leq \delta$ , then one should choose  $\Delta t$  and  $\Delta x$  to satisfy

$$\frac{\Delta t}{\varepsilon} = O(\delta), \quad \left(\frac{|\Delta x|}{\varepsilon}\right)^m = O(\delta \Delta t).$$

Again one finds this meshing strategy is consistent with that for the magnetic Schrödinger equation [9, equation (3.54)].

## 5. Conclusion

We present, to the best of our knowledge, the first numerical approach for the time-dependent Pauli equation for a 2-spinor in three space dimensions (note that in the presence of electromagnetic fields only three-dimensional equations make sense physically). We extend schemes for the scalar magnetic Schrödinger equation without spin term [7, 8, 9], thus proposing a four-term operator splitting method. We also analyze the convergence of the scheme and present proof of concept numerical experiments obtained with a Julia implementation of the method.

The results are fully workable for time-independent as well as simple time-dependent magnetic fields, but as of now are restricted to the linear case, i.e., for given external magnetic vector and scalar electric potentials.

Throughout this paper we highlight the similarities and analogies between the Pauli equation and the magnetic Schrödinger equation, at least in three-dimensional space, and kept our notation as closely tied to this analogy as the mathematics allows. Nevertheless, there are important differences in physical meaning and mathematical structure even for results which may at first glance seem fully analogous. One primary example of this is that in the Pauli equation, ‘charge’ or ‘mass’ is generally only conserved in the sum over spin up and spin down states. Physically this means that one may observe oscillations of various kinds between the two spinor components, as was briefly explored in the numerical experiments presented in this paper. For the numerics of the Pauli equation, this coupled nature of the spin up and spin down state equations means that any error bounds can only be valid for the sum of the two states, as any errors can and will propagate between spin up and spin down state solutions in each step. Given this fact, it is remarkable that the error bounds obtained for the linear Pauli equation are well-behaved under relatively mild assumptions.

An important question for applications is the extension of this method to the fully self-consistent system consisting of the Pauli equation coupled to a suitable first order  $O(\frac{1}{c})$  approximation of the Maxwell equations. The canonical choice would be the so-called Pauli–Poiswell system [4], the elliptic Poiswell system as a variant of the magnetostatic approximation of the Maxwell equations [19]. For this system, extensions of our

method should be possible while still obtaining sensible error bounds, at least on the physical observables of interest. This is part of ongoing research on numerical methods for nonlinear Pauli equations.

### Acknowledgments

We acknowledge support of the Austrian Science Fund (FWF) via the grants FWF DK W1245 and SFB F65, support from the Vienna Science and Technology Fund (WWTF) project MA16-066 "SEQUEX" and the Univ. Wien research platform MMM ("Mathematics-Magnetism-Materials").

### References

- [1] D. J. Griffiths, *Introduction to elementary particles*, 2nd, rev. ed., Wiley-VCH, 2011.
- [2] M. D. Schwartz, *Quantum field theory and the standard model*, Cambridge University Press, 2014.
- [3] N. J. Mauser, Semi-relativistic approximations of the Dirac equation: First and second order corrections, *Transport Theory Statist. Phys.* 29 (2000) 449–464.
- [4] N. Masmoudi, N. J. Mauser, The selfconsistent Pauli equation, *Monatsh. Math.* 132 (2001) 19–24.
- [5] M. Nowakowski, The quantum mechanical current of the Pauli equation, *Am. J. Phys.* 67 (1999) 916–919.
- [6] R. I. McLachlan, G. R. W. Quispel, Splitting methods, *Acta Numer.* 11 (2002) 341–434.
- [7] S. Jin, Z. Zhou, A semi-Lagrangian time splitting method for the Schrödinger equation with vector potentials, *Commun. Inf. Syst.* 13 (2013) 247–289.
- [8] M. Caliari, A. Ostermann, C. Piazzola, A splitting approach for the magnetic Schrödinger equation, *J. Comput. Appl. Math.* 316 (2017) 74–85.
- [9] Z. Ma, Y. Zhang, Z. Zhou, An improved semi-Lagrangian time splitting spectral method for the semi-classical Schrödinger equation with vector potentials using NUFFT, *Appl. Numer. Math.* 111 (2017) 144–159.
- [10] S. G. Johnson, Notes on FFT-based differentiation, 2011. <http://math.mit.edu/~stevenj/fft-deriv.pdf>.
- [11] J. Bezanson, A. Edelman, S. Karpinski, V. B. Shah, Julia: A fresh approach to numerical computing, *SIAM Rev.* 59 (2017) 65–98.
- [12] M. Thalhammer, High-Order Exponential Operator Splitting Methods for Time-Dependent Schrödinger Equations, *SIAM J. Numer. Anal.* 46 (2008) 2022–2038.

- [13] W. Bao, J. Shi, P. Markowich, On time-splitting spectral approximations for the Schrödinger equation in the semiclassical regime, *J. Comp. Phys.* 175 (2002) 487–524.
- [14] T. Jahnke, C. Lubich, Error bounds for exponential operator splittings, *BIT* 40 (2000) 735–744.
- [15] S. Descombes, M. Thalhammer, The Lie–Trotter splitting for nonlinear evolutionary problems with critical parameters: a compact local error representation and application to nonlinear Schrödinger equations in the semiclassical regime, *IMA J. Numer. Anal.* 33 (2013) 722–745.
- [16] M. Kapralov, A. Velingker, A. Zandieh, Dimension-independent Sparse Fourier Transform, 2019. arXiv:1902.10633.
- [17] E. Süli, A. Ware, A spectral method of characteristics for hyperbolic problems, *SIAM J. Numer. Anal.* 28 (1991) 423–445.
- [18] J. E. Pasciak, Spectral and pseudo spectral methods for advection equations, *Math. Comp.* 35 (1980).
- [19] N. Besse, N. Mauser, E. Sonnendrücker, Numerical Approximation of Self-Consistent Vlasov Models for Low-Frequency Electromagnetic Phenomena, *Int. J. Appl. Math. Comput. Sci.* 17 (2007) 361–374.